Industrial Crops and Products 85 (2016) 258–265

Contents lists available at ScienceDirect

Industrial Crops and Products

journal homepage: www.elsevier.com/locate/indcrop

Revealing the influences of cellulose on cellulose/SrF_2 nanocomposites synthesized by microwave-assisted method

Fu Deng[a,1], Yan-Yan Dong[a,1], Shan Liu[a], Bo Wang[a], Ming-Guo Ma[a,*], Xuan Du[b]

[a] Engineering Research Center of Forestry Biomass Materials and Bioenergy, Beijing Key Laboratory of Lignocellulosic Chemistry, College of Materials Science and Technology, Beijing Forestry University, Beijing 100083, PR China
[b] National Engineering Laboratory for Hydrometallurgical Cleaner Production Technology, Institute of Process Engineering, Chinese Academy of Sciences, Beijing 100190, PR China

ARTICLE INFO

Article history:
Received 10 May 2015
Received in revised form 1 March 2016
Accepted 9 March 2016
Available online 19 March 2016

Keywords:
Cellulose
Nanocomposites
SrF_2
Microwave
Tensile properties

ABSTRACT

The purpose of this article was to investigate the effect of the cellulose content on the synthesis of cellulose/SrF_2 nanocomposites, which were successfully synthesized by the microwave-assisted method at 100 °C for 20 min. These nanocomposites were investigated by X-ray powder diffraction (XRD), scanning electron microscopy (SEM), field emission scanning electron microscopy (FE-SEM), thermogravimetric analysis (TG), and derivative thermogravimetric (DTG). In addition to this, this synthetic route was also extended to fabricate the other cellulose/alkaline earth metal fluorides (MF_2, M = Ca, Mg, Ba) nanocomposites. What's more, the influence of cellulose/alkaline earth metal fluorides (MF_2, M = Ca, Mg, Sr, Ba) nanocomposites on the tensile properties of paper were also explored. The cellulose content is found to have a certain influence on the morphology, crystal lattice, crystallinity and thermostability of alkaline earth metal fluorides. The different types of alkaline earth metal fluorides have an effect on the tensile strength of paper.

1. Introduction

As the environmental problems become increasingly prominent, the properties of traditional materials are so limited that cannot satisfied people's needs, while functional nanocomposites are favored by many researchers. Cellulose, as one of the most abundant biopolymers, is widely used in various fields due to its unique properties such as stable chemical properties, good mechanical, excellent biocompatibility and biodegradability (André et al., 2009; István and David, 2010; Mtibe et al., 2015; Mithilesh et al., 2015). Nowadays, researchers devoted themselves to functional nanocomposites in order to make its properties better than individual component. Organic/inorganic nanocomposites with a brand-new appearance appeared and many researchers are full of enthusiasm about studying them (Balwinder and Rajendra, 2015; Barletta et al., 2015; Criado et al., 2014; Long et al., 2015; Zhang et al., 2015). Cellulose-based composites, as a member of the big family, are widely researched due to their advantages such as edibility, barrier properties, attractive appearance, biocompatibility, non-polluting, non-toxicity, and low cost (Imran et al., 2010; Márcia et al., 2012). There are a few reports on the various cellulose-based composites including cellulose/$CaCO_3$ (Ma et al., 2013), cellulose/hydroxyapatite (Yin et al., 2011), cellulose/SiO_2 (Gil et al., 2008), cellulose/titanium dioxide (Paula et al., 2006), and cellulose/Fe_3O_4 (Zhu et al., 2011).

Alkaline earth metal fluorides played an important role in the family of fluoride, which possessed excellent mechanical behavior, optical property, and mechanical stability (Ratnesh et al., 2014). The widely applications of alkaline earth metal fluorides have been investigated. For instance, magnesium fluoride nanoparticles were used to improve antibacterial and antibiofilm activity (Jonathan et al., 2012). Magnesium fluoride was added into Al_2O_3-MgO cement bonded castables to improve the overall performance of refractory castables at high temperature (Souza et al., 2014). The addition of CaF_2 into the nano-hydroxyapatite and titania composites was reported to improve the microhardness of composites (Isıl et al., 2014). Single-crystal calcium fluoride was used as high efficient optical micro-resonators (Shunya et al., 2014). More recently, titanium dioxide/calcium fluoride (TiO_2/CaF_2) photoanodes were applied as efficient dye-sensitized solar cell (Wang et al., 2015). Moreover, the phase and thermal behavior of strontium fluoride glass have also been researched (Christian et al., 2013; Reben, 2011). Strontium fluoride-loaded titania was used for azo

* Corresponding author.
E-mail address: mg_ma@bjfu.edu.cn (M.-G. Ma).
[1] These authors contributed equally to this work.

http://dx.doi.org/10.1016/j.indcrop.2016.03.018
0926-6690/

dye degradation (Subash et al., 2013). What's more, strontium fluoride combines with rare earth element were prepared for white light luminophores by co-precipitation method (Rozhnova et al., 2014). The barium fluoride-titanium dioxide nanocomposites were applied for the photodegradation of trypan blue dye (Velmurugan et al., 2014). Although alkaline earth metal fluorides compound inorganic matters were widely investigated, alkaline earth metal fluorides/organic nanocomposites have been little researched.

As an important class of fluorides, alkaline earth metal fluorides have wide potential applications in optics, biological labels and buffer layers in semiconductor-on-insulator structures. Cellulose/MF_2 (M = Ca, Mg, Sr, Ba) composites, which combined the advantages of both cellulose and inorganic nanoparticles, are mainly used in the manufacture of optical glass, advanced electronic components, etc. In addition, they can also be used in pharmaceutical and other substitute of fluoride. In the previous study, cellulose/alkaline earth metal fluorides nanocomposites were successfully synthesized by the microwave-assisted method using cellulose and cellulose solution pretreated with NaOH/urea (Deng et al., 2015a). Moreover, the influences of the different temperature, different heating-time, and different heating methods on the cellulose/alkaline earth metal fluorides nanocomposites were also investigated (Deng et al., 2015b). During the synthetic procedure, it was found that the cellulose played an important role in the cellulose/alkaline earth metal fluorides nanocomposites. However, the mechanism of cellulose on the nanocomposites is still not understood in depth and also needed to be further studied in detail. In this article, cellulose/SrF_2 nanocomposites were successfully synthesized by the microwave-assisted ionic liquid method at 100 °C for 20 min. The different cellulose concentrations perform significant influence on the crystallinity, crystal lattice, and morphology of strontium fluorides. The influence of different cellulose concentrations about the thermostability of strontium fluoride was also discussed. This synthetic route was extended to the other cellulose/alkaline earth metal fluorides (MF_2, M = Ca, Mg, Ba) nanocomposites. In the literature (Deng et al., 2015a,b), the cellulose/alkaline earth metal fluorides nanocomposites were synthesized via the microwave-assisted method in ionic liquid. However, in this paper, the influences of cellulose concentration on the cellulose/alkaline earth metal fluorides (MF_2, M = Ca, Mg, Sr, Ba) were investigated using ionic liquid as additive. The effect of cellulose/alkaline earth metal fluorides (MF_2, M = Ca, Mg, Sr, Ba) on the tensile strength of paper was also explored by adding nanocomposites into paper pulp to make paper. Herein, the cellulose composited with MF_2 (M = Ca, Mg, Sr, Ba) particles to fabricate cellulose/MF_2 (M = Ca, Mg, Sr, Ba) nanocomposites. It is well known that the major component of paper is cellulose. Such papers, consisted of alkaline earth metal fluorides/cellulose hybrids and paper pulp, can improve the property of paper. It is conducive to the development of paper industry. The introduce of alkaline earth metal fluorides can enhance the strength of the papers and have influences in the papers' cobb, tearing, wet strength, and internal cohesion, etc. The as-prepared papers have potential applications in medical health care, water treatment, and food packaging industry. Fig. 1 showed the schematic diagram of the formation process of cellulose/alkaline earth metal fluorides particles.

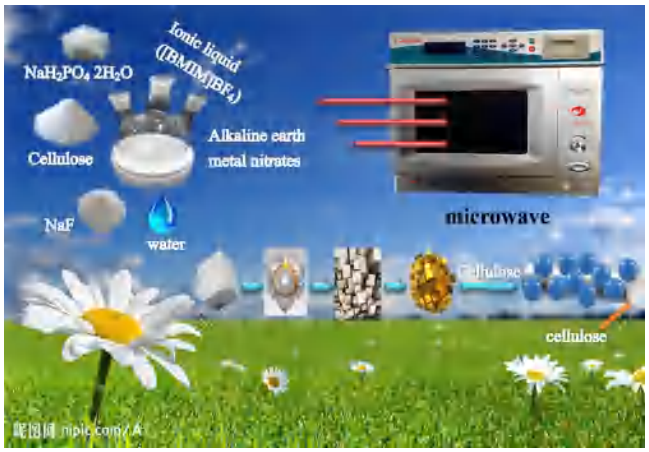

Fig. 1. The schematic diagram of the formation process of cellulose/alkaline earth metal fluorides particles.

2. Experimental

2.1. Materials

All chemicals were of analytical grade and used as received without further purification. All experiments were conducted under an air atmosphere. Microcrystalline cellulose (molecular weight of 34,843–38,894, degree of polymerization (DP, DP = 215–240)) of a commercial reagent was purchased from Sinopharm Group Chemical Reagent Co., Ltd., Shanghai, China. Calcium nitrate ($Ca(NO_3)_2$), magnesium nitrate ($Mg(NO_3)_2$), strontium nitrate ($Sr(NO_3)_2$), barium nitrate ($Ba(NO_3)_2$), sodium dihydrogen phosphate (NaH_2PO_4), and sodium fluoride (NaF) were purchased from Beijing Chemical Works.

2.2. Synthetic process of cellulose/SrF_2 nanocomposites

For the synthesis of cellulose/SrF_2 nanocomposites, microcrystalline cellulose (0.050 g), ionic liquid (2 mL) and sodium dihydrogen phosphate (NaH_2PO_4) (0.156 g) were added into three flask with deionized water (35 mL). Then, strontium nitrate (0.211 g) was directly dissolved into above-mentioned mixed solution, respectively. At last, sodium fluoride (0.084 g) was added in the mixed solution. The mixed solution was heated to 100 °C for 20 min in the microwave oven using 700W cyclic microwave radiation and then air cooled to room temperature (model: XH100A, Xiang Hu Science and Technology Development Co., Ltd, Beijing). The white products were obtained by centrifugal separation and washed with deionized water followed by ethanol for three times, and dried at 60 °C for further characterization.

For comparison, samples were also synthesized by the microwave-assisted method using different microcrystalline cellulose concentrations (0.10 g, 0.20 g, 0.40 g, 0.80 g). The dosage of other reagents and the other conditions are all kept the same.

2.3. Characterization

X-ray powder diffraction (XRD) patterns were performed in the 2θ range from 10° to 70° on a Rigaku D/Max 2200-PC diffractometer with Cu Kα radiation (λ = 0.15418 nm) and a graphite monochromator at ambient temperature. Scanning electron microscopy (SEM) images were obtained with a Hitachi 3400 N scanning electron microscopy. All samples were Au coated prior to examination by SEM and cellulose/SrF_2 were investigated by F-SEM. Thermal behavior of the samples was tested using thermogravimetric (TG) and differential thermal gravity (DTG) on a simultaneous thermal analyzer (DTG-60, Shimadzu) at a heating rate of 10 °C min^{-1} in flowing air.

3. Results and discussion

The XRD patterns of cellulose/SrF_2 nanocomposites were showed in Fig. 2, which were synthesized by the microwave-assisted method at 100 °C for 20 min using 0.05 g, 0.10 g, 0.20 g,

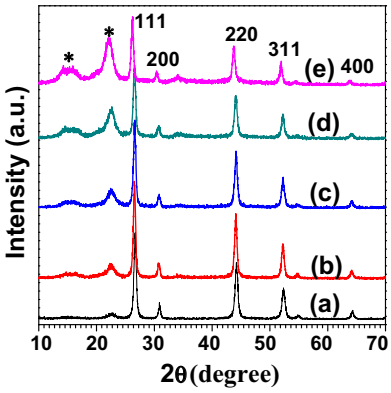

Fig. 2. XRD patterns of the cellulose/SrF_2 nanocomposites prepared via microwave-assisted method at 100 °C for 20 min using: (a) 0.05 g cellulose, (b) 0.1 g cellulose, (c) 0.2 g cellulose, (d) 0.4 g cellulose, (e) 0.8 g cellulose.

0.40 g, and 0.80 g cellulose, respectively. The characteristic peaks of cellulose were marked with *in Fig. 2, which increased with increasing cellulose contents. The characteristic peaks of SrF_2 were also showed such as the planes of (111), (200), (220), (311), and (400). When the cellulose content increased from 0.05 g to 0.80 g, the peaks intensities slightly increased first, then decreased with increasing cellulose contents, indicating the change crystallinity of SrF_2 crystals.

Fig. 3 showed the morphologies of cellulose/SrF_2 nanocomposites with SEM and FE-SEM. When 0.05 g cellulose was used as matrix, one can see plentiful of SrF_2 spherical particles evenly distributed on the cellulose strip (Fig. 3a). Seeing from the magnification image of individual SrF_2 spherical (the down set of Fig. 3a), one can conclude that the big SrF_2 spherical was formed by amounts of SrF_2 nanoparticles. Increasing the cellulose concentration to 0.10 g cellulose, amounts of SrF_2 particles adhered to cellulose strip (Fig. 3b). As shown in the set of Fig. 3b, the surface of SrF_2 particles became slightly smooth and the size decreased mildly, compared with Fig. 3a. When the cellulose content increased to 0.20 g, one can clearly see that the size of SrF_2 particles obviously decreased (Fig. 3c). The magnification image showed that the SrF_2 particles performed more smoothly. The sample displayed a similar shape using 0.40 g cellulose, as shown in Fig. 3d. When the cellulose con-

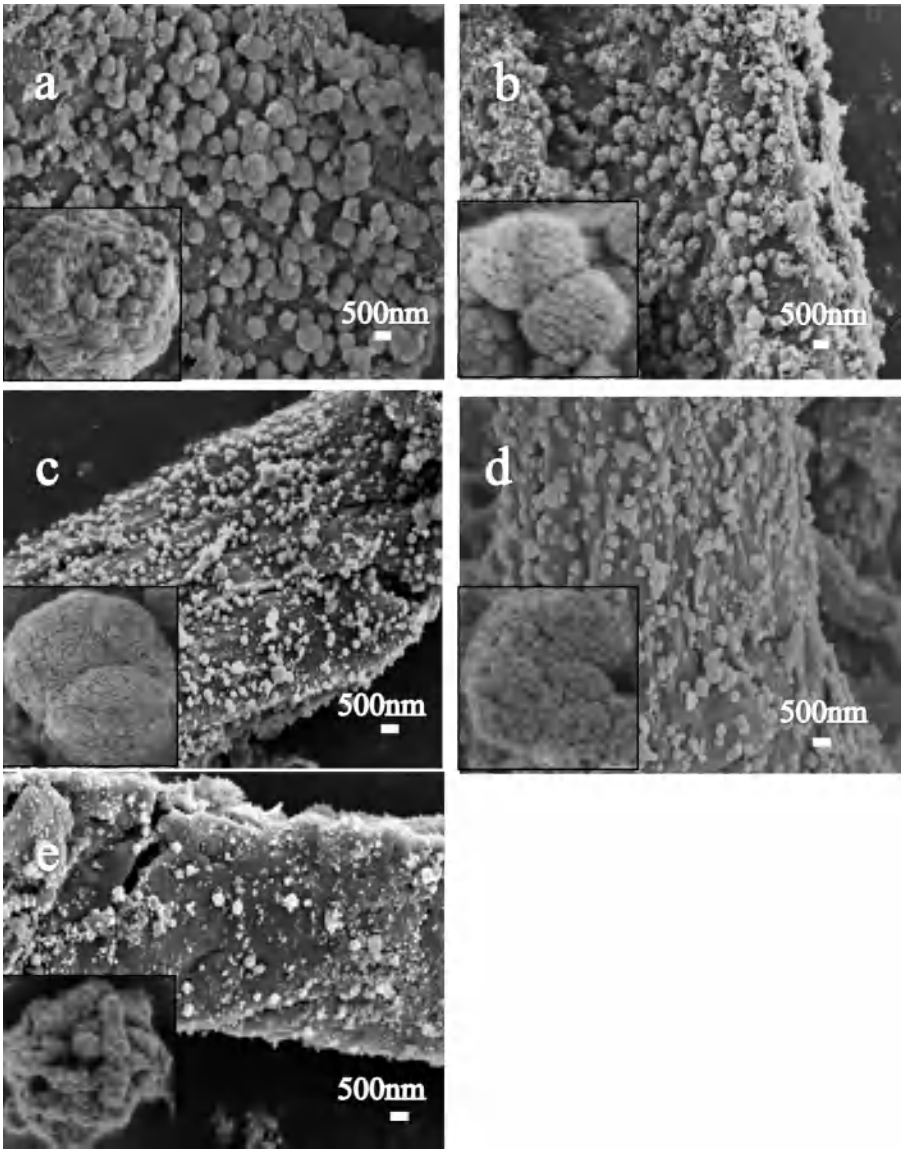

Fig. 3. SEM and FE-SEM images of the cellulose/SrF_2 nanocomposites prepared via microwave-assisted method at 100 °C for 20 min using: (a) 0.05 g cellulose, (b) 0.1 g cellulose, (c) 0.2 g cellulose, (d) 0.4 g cellulose, (e) 0.8 g cellulose.

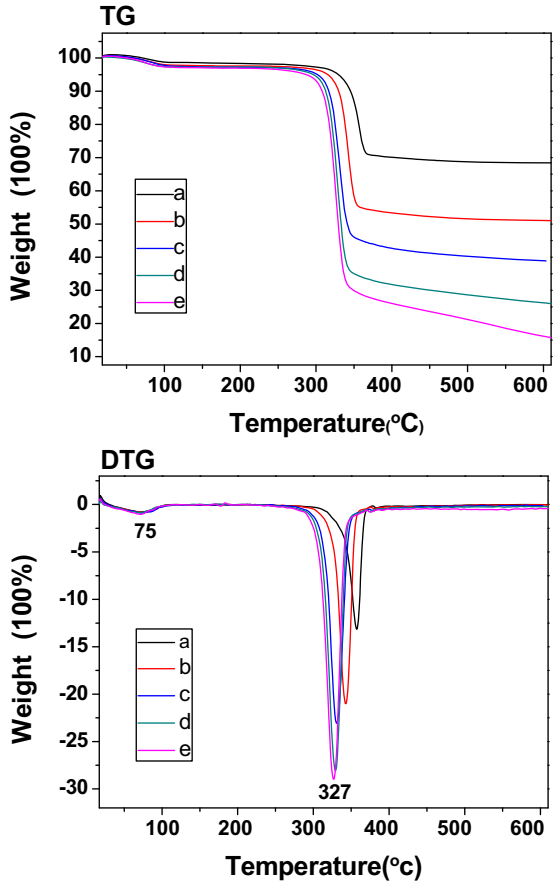

Fig. 4. TG and DTG curves of the cellulose/SrF_2 nanocomposites prepared via microwave-assisted method at 100 °C for 20 min using: (a) 0.05 g cellulose, (b) 0.1 g cellulose, (c) 0.2 g cellulose, (d) 0.4 g cellulose, (e) 0.8 g cellulose.

tent reached to 0.80 g, one can see that the quantity of SrF_2 particles decreased and the size of SrF_2 particles was not uniform (Fig. 3e). It also observed that some SrF_2 particles aggregated to form irregular spheres. These images showed a large number of tiny particles of strontium fluorides particles self-assemble to form the larger particles. But the quantity of particles, the size of particles, the shape of particles and the combining degree between particles changed, indicating that cellulose content had a certain influence on the morphology of SrF_2. The size distributions for the SrF_2 particles in the cellulose/SrF_2 nanocomposites synthesized with different dosages of cellulose were shown in Fig. S1(a–c). The average sizes of SrF_2 particles are 255 nm, 251 nm, and 162 nm using cellulose concentrations of 0.05 g, 0.2 g, and 0.8 g, respectively. Based on the results, the SrF_2 particles synthesized with 0.8 g of cellulose have the uniform size distribution.

The thermal behavior of cellulose/SrF_2 nanocomposites was also investigated with TG and DTG, as shown in Fig. 4. As for cellulose/SrF_2 nanocomposites synthesized by the microwave-assisted method at 100 °C for 20 min using 0.05 g, 0.10 g, 0.20 g, 0.40 g, and 0.80 g cellulose, the total weight losses of cellulose/SrF_2 nanocomposites were 31.6%, 47.6%, 61.1%, 73.7% and 83.6%, respectively. The weight loss was mainly attributed to the loss of cellulose, according with the endothermic peak located at 327 °C. On the other hand, corresponding to the percentage content of cellulose are 32.1%, 48.6%, 65.4%, 79.1%, and 88.4%, respectively. These results manifested that the amount of remaining cellulose gradually increased, indicating that the combining capacity between cellulose and SrF_2 increased with increasing cellulose content. Obviously, cellulose content had influence on the thermal stability of cellulose/SrF_2 nanocomposites. Seeing in TG curves, a small weight loss around 25–100 °C was contributed to the desorption water, accompanied by an endothermic peak at about 75 °C in DTG curves.

This synthetic route was also applied for the synthesis of the other cellulose/alkaline earth metal fluorides (MF_2, M = Ca, Mg, Ba) nanocomposites. The XRD patterns of cellulose/CaF_2 nanocomposites were showed in Fig. 5, which were also synthesized by the microwave-assisted method at 100 °C for 20 min using 0.05 g, 0.10 g, 0.20 g, 0.40 g, and 0.80 g cellulose, respectively. One can clearly see the characteristic peaks of CaF_2 and cellulose (marked with * in Fig. 5a–e). The peaks intensities of cellulose increased with increasing cellulose contents, which are similar with cellulose/SrF_2 nanocomposites. However, the peaks intensities such as the planes of (111), (220), (311), and (400) of CaF_2 increased first, then decreased with increasing cellulose contents. These results indicated that the cellulose content indeed had significant influence on the crystallinity of CaF_2. When 0.05 g cellulose was used, the peaks shift occurred, which may be result from the change crystal lattice of CaF_2 (Fig. 5a). As shown in Fig. 5c, one can observe that the highest peaks of CaF_2 were obtained using 0.20 g cellulose. Fig. 5f–j showed the corresponding SEM micrographs of cellulose/CaF_2 nanocomposites. One can see amount of CaF_2 particles grew on cellulose matrix and the significantly changed size of CaF_2 particles. Using 0.05 g cellulose, the morphology of CaF_2 particles performer ruleless (Fig. 5f). Increasing the cellulose content to 0.10 g, one can also see amounts of CaF_2 nanoparticles with nonuniform size scattered in cellulose strip (Fig. 5g). When the cellulose content was increased to 0.20 g, the CaF_2 sphericals with big size were well-distributed (Fig. 5h). Using 0.40 g cellulose, sub-size CaF_2 particles gather together, result in the different sizes (Fig. 5i). What's more, one can see many CaF_2 sphericals using 0.80 g cellulose (Fig. 5j).

Cellulose/MgF_2 nanocomposites were synthesized by the microwave-assisted method at 100 °C for 20 min using 0.05–0.80 g cellulose, respectively. The corresponding XRD patterns of nanocomposites were shown in Fig. 6a–e. One can see that cellulose content had significant effect on the crystallinity of MgF_2. The peaks intensities of cellulose increased with the increasing cellulose contents (marked with * in Fig. 6a–e). The characteristic peaks of MgF_2 such as the planes of (110), (101), (111), (210), (211), (220), and (301) were marked. Due to the effect of cellulose concentrations, some characteristic peaks of MgF_2 are too weak to observe, result in the different crystalline of MgF_2 crystals. A slight peaks shift of nanocomposites occurred using 0.80 g cellulose (Fig. 6e), which may be due to the change crystal lattice of MgF_2 crystals. Using 0.05 g cellulose, one can see that amounts of MgF_2 particles with different size covered on the surface of cellulose strip (Fig. 6f). When the cellulose content achieved 0.20 g, large amounts of MgF_2 particles homodispersed in cellulose strip (Fig. 6h). What's more, the size and morphology of large quantity MgF_2 particles were too small to see using 0.40 g cellulose (Fig. 6i). When the cellulose content changed to 0.80 g, one can see the MgF_2 particles with significantly reduced size (Fig. 6j). These results demonstrated that cellulose content had significant influence on both the morphology and dispersity of MgF_2 crystals.

Fig. 7a–e showed the XRD patterns of cellulose/BaF_2 nanocomposites synthesized using microwave-assisted at 100 °C for 20 min using different cellulose contents, respectively. One can clearly see the characteristic peak of cellulose (marked with *) and the characteristic peaks of BaF_2 such as the planes of (111), (200), (220), and (311). Obviously, the peak intensity of cellulose increased with increasing cellulose contents, while the peak intensity of BaF_2 decreased with increasing contents, implying that the more cellulose contents, the lower crystalline of BaF_2. The morphology of cellulose/BaF_2 nanocomposites was studied via SEM, as shown in Fig. 7f–j. Using 0.05 g cellulose, plenty of irregular BaF_2 particles

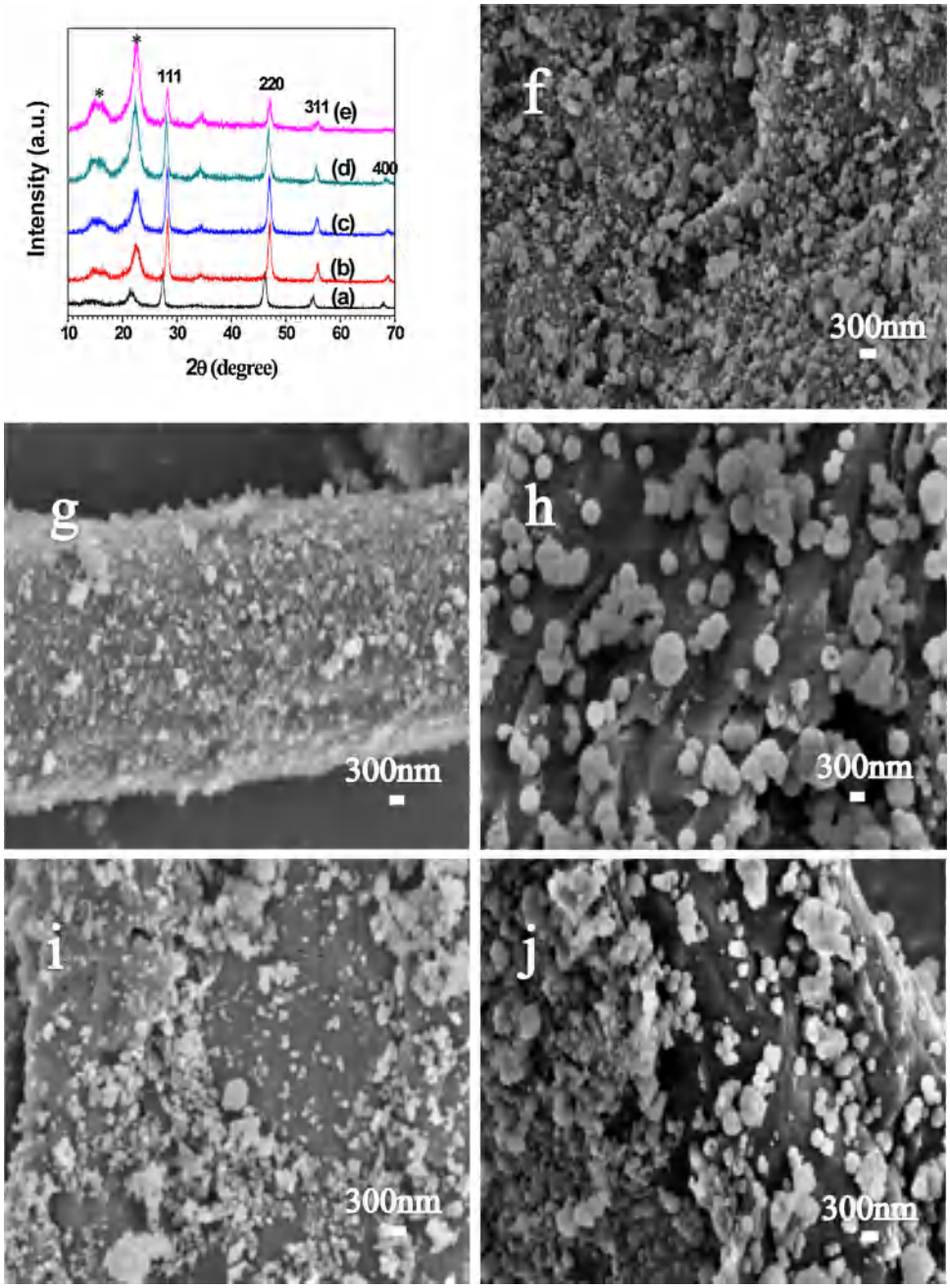

Fig. 5. XRD patterns (a–e) and SEM images (f–j) of the cellulose/CaF_2 nanocomposites prepared via microwave-assisted method at 100 °C for 20 min using: (a and f) 0.05 g cellulose, (b and g) 0.1 g cellulose, (c and h) 0.2 g cellulose, (d and i) 0.4 g cellulose, (e and j) 0.8 g cellulose.

scattered on the cellulose strip (Fig. 7f). One can infer BaF_2 particles wrapped around cellulose liking a layer of film. When the cellulose content increased, the quantity of BaF_2 particles decreased (Fig. 7f–j). The results exhibited that quantities of BaF_2 particles as a membrane covered the surface of cellulose and only irregular BaF_2 particles could be seen. Normally, BaF_2 is a cubic crystal structure. The shape of BaF_2 particles in performed ruleless, demonstrating that cellulose contents had influence on the shape of BaF_2 particles. This may be due to the increasing ionic radius, which caused a reduction of action force between the particles, and then affecting the self-assembly between particles. Moreover, the dispersity of BaF_2 particles perform well and the quantity of BaF_2 particles decreased with increasing cellulose content.

Fig. 8 showed the brief schematic diagram of the process of paper-making. The cellulose/alkaline earth metal fluorides (MF_2, M = Ca, Mg, Sr, Ba) nanocomposites were put into the paper pulp, stir evenly, and then made by the standard of sheet forming system, which included sheer shaper, squeezing device, paper exposing device and dryers. The paper with 1.88 g was put into desiccator for 24 h.

The effect of cellulose/alkaline earth metal fluorides (MF_2, M = Ca, Mg, Sr, Ba) nanocomposites on tensile properties of paper was also investigated, as shown in Fig. 9. The cellulose/alkaline earth metal fluorides nanocomposites were synthesized by the microwave-assisted method at 100 °C for 20 min using 0.20 g cellulose. The traditional paper-making process were used, every paper own the same weight. In comparison with the control of blank sample, one can see the increased tensile properties. The tensile index increased by 17.5% for cellulose/CaF_2, 29.4% for cellulose/MgF_2, 32.8% for cellulose/SrF_2, 40.4% for cellulose/BaF_2 nanocomposites,

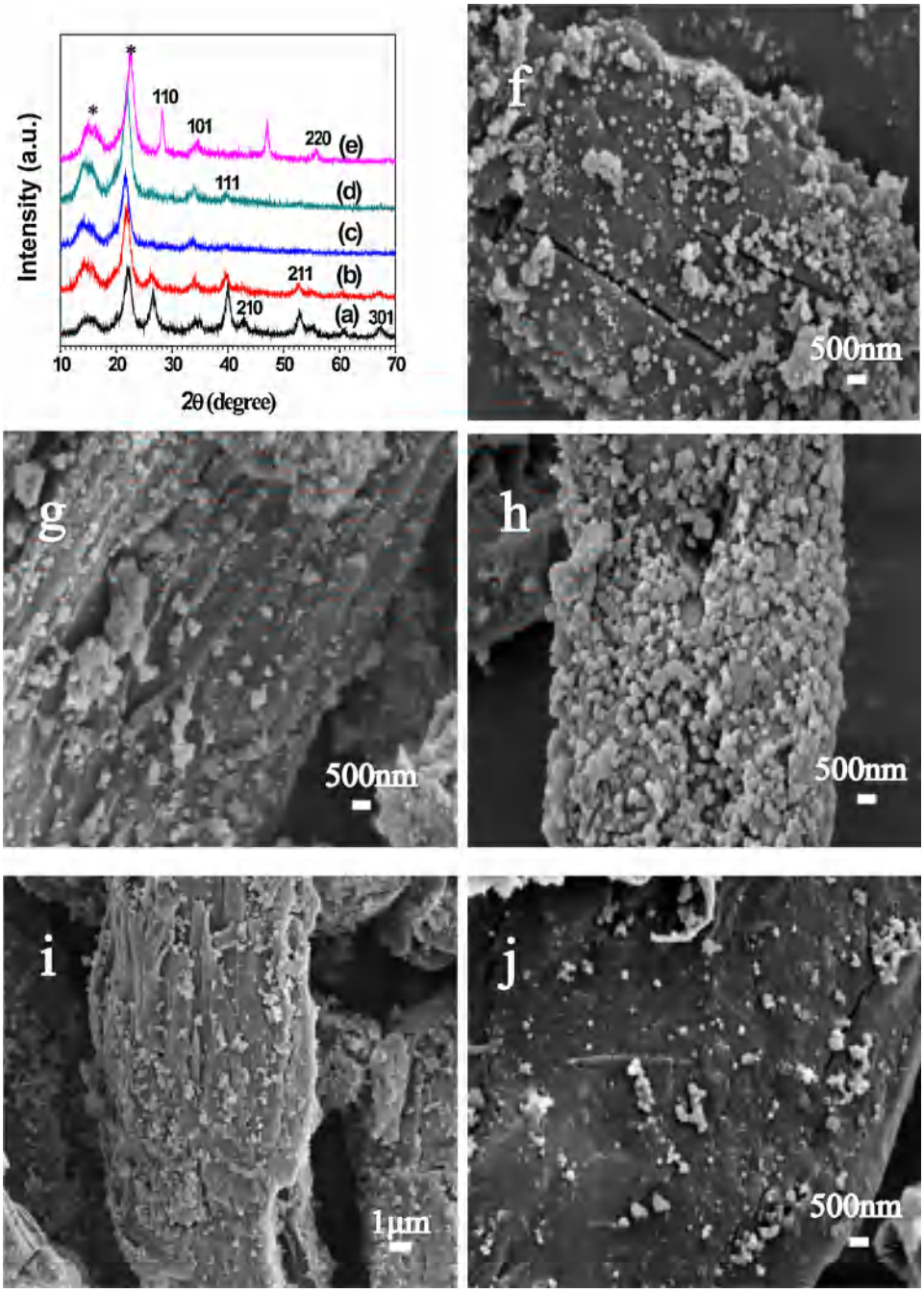

Fig. 6. XRD patterns (a–e) and SEM images (f–j) of the cellulose/MgF_2 nanocomposites prepared via microwave-assisted method at 100 °C for 20 min using: (a and f) 0.05 g cellulose, (b and g) 0.1 g cellulose, (c and h) 0.2 g cellulose, (d and i) 0.4 g cellulose, (e and j) 0.8 g cellulose.

respectively. These results demonstrated that cellulose/alkaline earth metal fluorides nanocomposites had significant influence on the tensile properties of paper. On the other hand, the alkaline earth metal fluorides played different nature on the tensile properties of paper, which may result from the different filling capacity in pores of paper and different covalent and hydrogen boning ability. Moreover, we also investigated the cobb value, tearing resistance, and wet strength of samples. The control of blank sample displayed the cobb value, tearing resistance, and wet strength of 31.80 g/m^2, 210 mN, and 24.1 N, respectively. As for the cellulose/SrF_2 nanocomposites, the cobb value, tearing resistance, and wet strength increased to 39.95 g/m^2, 243 mN, and 26.4 N, respectively. One can observe the cobb value of 54.62 g/m^2, tearing resistance of 281 mN, and wet strength of 30.2 N for the cellulose/BaF_2 nanocomposites, respectively. Furthermore, the zeta potential of the pulp is −40.3 mV.

In the literature, silver particles filled cellulose hybrids were synthesized using microcrystalline cellulose solution by a hydrothermal method (Dong et al., 2015). The Ag^+ release concentrations were 0.091 ppm, 0.073 ppm, and 0.080 ppm using H_2O as solvent for 4, 12, and 24 h, respectively. The cellulose/alkaline earth metal fluorides (MF_2, M = Ca, Mg, Ba) nanocomposites are also important biomedical materials. Therefore, the release of metallic particles is of great importance for the applications of the cellulose/alkaline earth metal fluorides (MF_2, M = Ca, Mg, Ba) nanocomposites. However, in this paper, the cellulose/MF_2 (M = Ca, Mg, Sr, Ba) composites were obtained in the deionized and the MF_2 (M = Ca, Mg, Sr, Ba) particles were attached on the surface

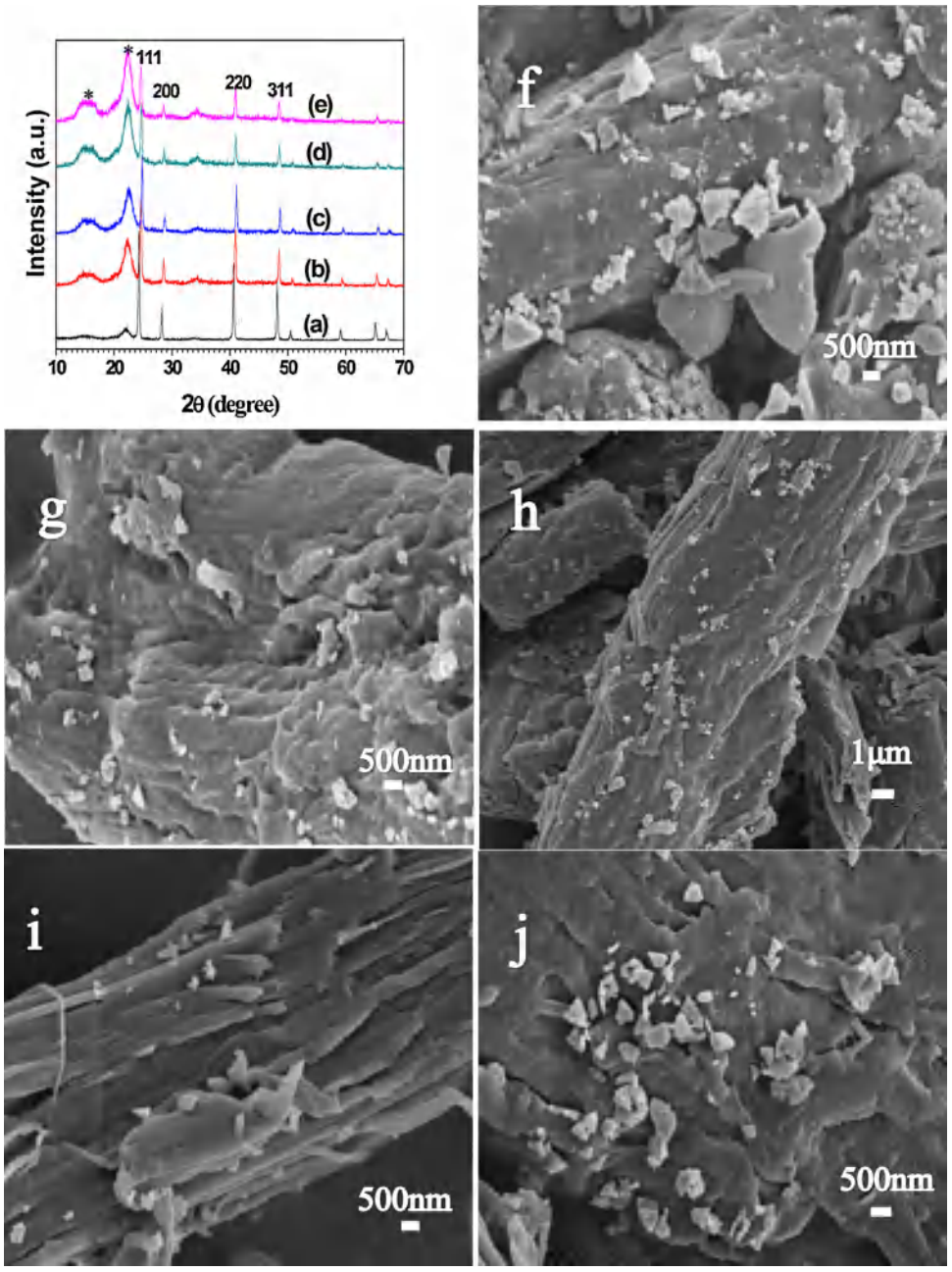

Fig. 7. XRD patterns (a–e) and SEM images (f–j) of the cellulose/BaF_2 nanocomposites prepared via microwave-assisted method at 100 °C for 20 min using: (a and f) 0.05 g cellulose, (b and g) 0.1 g cellulose, (c and h) 0.2 g cellulose, (d and i) 0.4 g cellulose, (e and j) 0.8 g cellulose.

Fig. 8. The brief schematic diagram of the process of the paper-making.

of cellulose, which could restrain the release of MF_2 (M = Ca, Mg, Sr, Ba) in the cellulose composites. Biomass is the most abundant renewable resources for human beings. Developing and utilizing biomass scientifically is an important way of sustainable development. Biorefinery can environmentally friendly convert biomass to high value-added multiple bioproducts and bioenergy. The refining of cellulose reported in this article revealed that nanocomposites of cellulose/alkaline earth metal fluorides (MF_2, M = Ca, Mg, Sr,

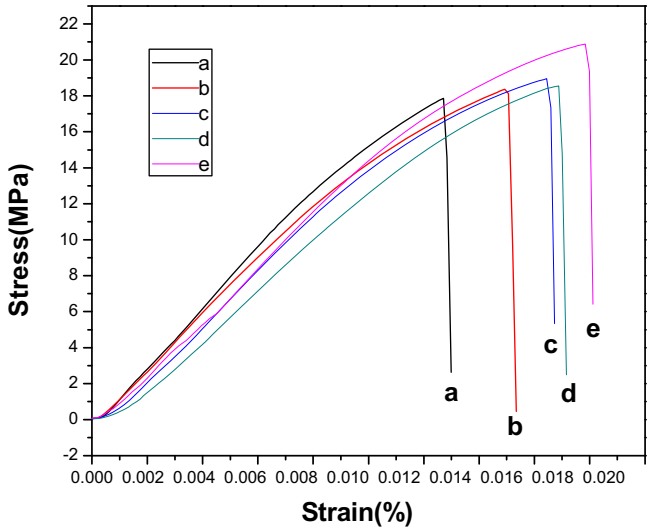

Fig. 9. The stress-strain curves of papers adding cellulose/alkaline earth metal fluorides (MF_2, M = Ca, Mg, Sr, Ba) nanocomposites which were synthesized by microwave-assisted method at 100 °C for 20 min using 0.2 g cellulose: (a) blank sample, (b) cellulose/CaF_2, (c) cellulose/MgF_2, (d) cellulose/SrF_2, (e) cellulose/BaF_2.

Ba) have potential application in enhancing the tensile strength of papers.

4. Conclusions

In summary, cellulose/SrF_2 nanocomposites were successfully synthesized by the microwave-assisted method using different cellulose concentrations. The different cellulose contents played an important role on the morphology, crystal lattice, crystallinity of nanocomposites. The cellulose contents also performed certain influence on the thermostability of cellulose/SrF_2 nanocomposites. The influences of cellulose on the other cellulose/alkaline earth metal fluorides (MF_2, M = Ca, Mg, Ba) nanocomposites were also explored. The different types of alkaline earth metal fluorides had an effect on the tensile strength of paper.

Acknowledgments

Financial support from the Fundamental Research Funds for the Central Universities (No. JC2013-3) and National Natural Science Foundation of China (51302264) is gratefully acknowledged.

Appendix A. Supplementary data

Supplementary data associated with this article can be found, in the online version, at http://dx.doi.org/10.1016/j.indcrop.2016.03.018.

References

André, P., Kenneth, N.M., Pang, S.S., Mark, P.S., 2009. Ionic liquids and their interaction with cellulose. Chem. Rev. 109, 6712–6728.
Balwinder, K., Rajendra, S., 2015. Simultaneous determination of epinephrine paracetamol, and folicacid using transition metal ion-exchanged polyaniline-zeoliteorganic-inorganic hybrid materials. Sens. Actuators B-Chem. 211, 476–488.
Barletta, M., Gisario, A., Puopolo, M., Vesco, S., 2015. Scratch: wear and corrosion resistant organic inorganic hybrid materials for metals protection and barrier. Mater. Des. 69, 130–140.
Christian, B., Janine, W., Christian, R., 2013. The formation of strontium fluoride nano crystals from a phase separated silicate glass. J. Eur. Ceram. Soc. 33, 1737–1745.
Criado, M., Sobrados, I., Sanz, J., 2014. Polymerization of hybrid organic-inorganic materials from several silicon compounds followed by TGA/DTA, FTIR and NMR techniques. Prog. Org. Coat. 77, 880–891.
Deng, F., Fu, L.H., Ma, M.G., 2015a. Microwave-assisted rapid synthesis and characterization of CaF_2 particles-filled cellulose nanocomposites in ionic liquid. Carbohyd. Polym. 121, 163–168.
Deng, F., Fu, L.H., Zhang, X.M., Ma, M.G., 2015b. Comparative study on the nanocomposites of cellulose and alkali earth metal fluorides (MF_2, M=Ca, Mg, Sr, Ba) via microwave-assisted method. Sci. Adv. Mater. 7, 509–517.
Dong, Y.Y., Fu, L.H., Liu, S., Ma, M.G., Wang, B., 2015. Silver-reinforced cellulose hybrids with enhanced antibacterial activity: synthesis, characterization, and mechanism. RSC. Adv. 5, 97359–97366.
Gil, G., Paula, A.A.P.M., Tito, T., Carlos, P.N., Alessandro, G., 2008. Superhydrophobic cellulose nanocomposites. J. Colloid. Interface Sci. 324, 42–46.
Imran, M., El-Fahmy, S., Revol-Junelles, A.M., Desobry, S., 2010. Cellulose derivative based active coatings: effects of nisin and plasticizer on physico-chemical and antimicrobial properties of hydroxypropyl methylcellulose films. Carbohyd. Polym. 81, 219–225.
Isıl, K., Bengi, Y., Zafer, E., Metin, U., 2014. Effect of calcium fluoride on mechanical behavior and sinterability of nano-hydroxyapatite and titania composites. Ceram. Int. 40, 14817–14826.
István, S., David, P., 2010. Microfibrillated cellulose and new nanocomposite materials: a review. Cellulose 17, 459–494.
Jonathan, L., Alexandra, F., Jean-Paul, L., Aharon, G., Ehud, B., 2012. Improved antibacterial and antibiofilm activity of magnesium fluoride nanoparticles obtained by water-based ultrasound chemistry. Nanomed. Nanotechnol. 8, 702–711.
Long, L., Liu, W.J., Xia, H.H., Ken, Y., Kawaguchi, T., Shimazu, K., 2015. Surface plasmon resonance investigation of two-dimensional organic–inorganic hybrid materials with mouse IgG. Sens. Actuators B-Chem. 213, 248–251.
Márcia, R.M., Luiz, H.C.M., Valtencir, Z., 2012. Development of cellulose-based bactericidal nanocomposites containing silver nanoparticles and their use as active food packaging. J. Food Eng. 109, 520–524.
Ma, M.G., Dong, Y.Y., Fu, L.H., Li, S.M., Sun, R.C., 2013. Cellulose/$CaCO_3$ nanocomposites microwave ionic liquid synthesis, characterization, and biological activity. Carbohyd. Polym. 92, 1669–1676.
Mithilesh, Y., Seongcheol, M., Jinho, H., Jaehwan, K., 2015. Synthesis and characterization of iron oxide/cellulose nanocomposite film. Int. J. Biol. Macromol. 74, 142–149.
Mtibe, A., Linda, Z.L., Mathew, A.P., Oksman, K., Maya, J.J., Rajesh, D.A., 2015. A comparative study on properties of micro and nanopapers produced from cellulose and cellulose nanofibers. Carbohyd. Polym. 118, 1–8.
Paula, A.A.P.M., Tito, T., Carlos, P.N., 2006. Titanium dioxide/cellulose nanocomposites prepared by a controlled hydrolysis method. Compos. Sci. Technol. 66, 1038–1044.
Ratnesh, K.P., Kevin, W., Sandeep, N., Hai, Y.H., Subhash, S.P., Avinash, C.P., Ravindra, P., 2014. A theoretical study of structural and electronic properties of alkaline-earth fluoride clusters. Comput. Theor. Chem. 1043, 24–30.
Reben, M., 2011. The thermal study of oxyfluoride glass with strontium fluoride. J. Non-Cryst. Solids 357, 2653–2657.
Rozhnova, Y.A., Luginina, A.A., Voronov, V.V., Ermakov, R.P., Kuznetsov, S.V., Ryabova, A.V., Pominova, D.V., Arbenina, V.V., Osiko, V.V., Fedorov, P.P., 2014. White light luminophores based on Yb^{3+}/Er^{3+}/Tm^{3+}-coactivated strontium fluoride powders. Mater. Chem. Phys. 148, 201–207.
Shunya, A., Kudo, H., Takasumi, T., Yan, J.W., Yasuhiro, K., 2014. Experimental analysis of the surface integrity of single-crystal calcium fluoride caused by ultra-precision turning. Procedia CIRP 13, 225–229.
Souza, T.M., Luz, A.P., Pandolfelli, V.C., 2014. Magnesium fluoride role on alumina-magnesia cement-bonded castables. Ceram. Int. 40, 14947–14956.
Subash, B., Krishnakumar, B., Velumurugan, R., Balachandran, S., Swaminathan, M., 2013. An efficient nanosized strontium fluoride-loaded titania for azo dye (RY 84) degradation with solar light. Mater. Sci. Semicon. Process. 16, 859–867.
Velmurugan, R., Krishnakumar, B., Swaminathan, M., 2014. Sonochemical synthesis and characterization of barium fluoride–titanium dioxide nanocomposites and activity for photodegradation of Trypan Blue dye. Mater. Sci. Semicon. Process. 27, 654–664.
Wang, Z.B., Tang, Q.W., He, B.L., Chen, X.X., Chen, H.Y., Yu, L.M., 2015. Titanium dioxide/calcium fluoride nanocrystallite for efficient dyesensitized solar cell: a strategy of enhancing light harvest. J. Power Sour. 275, 175–180.
Yin, N., Chen, S.Y., Yang, Y.O., Tang, L., Yang, J.X., Wang, H.P., 2011. Biomimetic mineralization synthesis of hydroxyapatite bacterial cellulose nanocomposites. Prog. Nat. Sci. 21, 472–477.
Zhang, Y., Guo, M., Pan, G.Y., Yan, H., Xu, J., Shi, Y.T., Shi, H.W., Liu, Y.Q., 2015. Preparation and properties of novel PH-stable TFC membrane based on organic–inorganic hybrid composite materials for nanofiltration. J. Membr. Sci. 476, 500–507.
Zhu, H.X., Jia, S.R., Wang, T., Jia, Y.Y., Yang, H.J., Li, J., Yan, L., Zhong, C., 2011. Biosynthesis of spherical Fe_3O_4/bacterial cellulose nanocomposites as adsorbents for heavy metal ions. Carbohyd. Polym. 86, 1558–1564.